

Accelerated escape dynamics in non-Markovian stochastic feedback

Francesco Coghi*

School of Physics and Astronomy, University of Nottingham, Nottingham NG7 2RD, United Kingdom and Nordita, KTH Royal Institute of Technology and Stockholm University, SE-106 91 Stockholm, Sweden

Romain Duvezin

Université Paris Saclay, ENS Paris Saclay, 91190 Gif-sur-Yvette, France and Nordita, KTH Royal Institute of Technology and Stockholm University, SE-106 91 Stockholm, Sweden

John S. Wettlaufer†

Yale University, New Haven, 06520, CT, USA and Nordita, KTH Royal Institute of Technology and Stockholm University, SE-106 91, Stockholm, Sweden

(Dated: May 15, 2025)

We study the escape dynamics of a non-Markovian stochastic process with time-averaged feedback, which we model as a one-dimensional Ornstein–Uhlenbeck process wherein the drift is modified by the empirical mean of its trajectory. This process maps onto a class of self-interacting diffusions. Using weak-noise large deviation theory, we derive the most probable escape paths and quantify their likelihood via the action functional. We compute the feedback-modified Kramers rate and its inverse, which approximates the mean escape time, and show that the feedback accelerates escape by storing finite-time fluctuations thereby lowering the effective energy barrier, and shifting the optimal escape time from infinite to finite. Although we identify alternative mechanisms, such as slingshot and ballistic escape trajectories, we find that they remain sub-optimal and hence do not accelerate escape. These results show how memory feedback reshapes rare event statistics, thereby offering a mechanism to potentially control escape dynamics.

I. INTRODUCTION

Many real-world systems exhibit memory-feedback dynamics [1–4], where the evolution of a process depends on its past trajectory. Unlike standard Markovian systems, these processes are influenced by accumulated memory. Such feedback mechanisms introduce rich dynamical features, altering long-time behavior and fluctuation properties in ways not captured by memoryless models [5–13]. In particular, memory-feedback mechanisms are relevant for designing control strategies to achieve specific tasks [14–18] with specific thermodynamic properties [19–25].

Self-interacting systems [26–32] constitute a notable class of memory-feedback processes in which past states, encoded in the empirical occupation measure, or in a time-integrated functional of the process, influence future evolution. Examples include models in statistical physics relevant to biological [33–37] and colloidal systems [38–40], where interactions with the occupation measure affect the dynamics.

Although the stationary properties of self-interacting processes have been studied extensively, the role of feedback in shaping rare event statistics, and in particular escape dynamics, remains poorly understood. However, understanding the finite-time stochastic dynamics of feedback-driven systems has many important implications in, among other problems, reinforcement learning algorithms [14].

Only recently have large-deviation results for self-interacting systems begun to emerge, both in the long-time regime for discrete Markov chains [41, 42] and for diffusions [43]. For example, escape dynamics has been addressed in self-interacting discrete-time random walks [44], where universal scaling laws for escape time distributions were identified, and in diffusive systems [45], where by analyzing the asymptotic behavior of the escape time in the weak-noise limit, a Kramers-type law was derived.

Here we analyze a representative case: a one-dimensional Ornstein–Uhlenbeck process where the drift term is influenced by its own time-averaged position. This feedback mechanism breaks Markovianity and defines a self-interacting diffusion process, fundamentally altering the escape dynamics of the system.

By using weak-noise large deviation theory, we show that self-interaction can lead to accelerated escape, and thus fluctuation-driven mechanisms induced by memory. In particular, we identify and characterize different escape scenarios and quantify their likelihood. Our large deviation approach allows us to derive a Kramers-type law for the mean escape time in the feedback Ornstein–Uhlenbeck process, which complements and extends the results in [44, 45]. Furthermore, our findings generalize recent results on escape dynamics in other classes of memory-driven systems, such as generalized Langevin equations [46, 47].

The paper is organized as follows. In Section II, we introduce the Ornstein–Uhlenbeck process with empirical average position feedback, establish its mapping to self-interacting diffusion, and discuss its deterministic and

* francesco.coghi@nottingham.ac.uk

† john.wettlaufer@yale.edu/jw@fysik.su.se

long-time dynamics. In Section III, we present the weak-noise large deviation framework used to derive our results. We apply it to both the standard and feedback Ornstein–Uhlenbeck processes, and derive the fundamental equation (59) governing finite-time dynamics in the weak-noise regime, which we have not found in the literature. In Section IV, we detail the consequences of solving (59). We describe the finite-time mechanisms driving escape in the feedback process, compare them to the standard Ornstein–Uhlenbeck case, and analyze their relative and absolute likelihoods. We characterize the quasi-potential (i.e., the large deviation rate function associated with the Arrhenius law) and the optimal escape times. Finally, in Section V we summarize our findings, highlight open questions, and discuss potential applications, particularly in the context of reinforcement learning.

II. STOCHASTIC FEEDBACK ORNSTEIN–UHLENBECK PROCESSES AND DETERMINISTIC DYNAMICS

A. Ornstein–Uhlenbeck Process with Empirical Average Position Feedback

We consider a one-dimensional process $(X_t)_{t \geq 0}$ governed by the following stochastic differential equation (SDE):

$$dX_t = -X_t dt + \frac{\beta}{t} \left(\int_0^t X_s ds \right) dt + \sqrt{\epsilon} dW_t, \quad (1)$$

with initial condition $X_0 = 0$, noise intensity $\epsilon > 0$, and feedback parameter $\beta \in (-\infty, 1)$, the range of which we will justify in detail below. Here, W_t denotes a standard Wiener process, or Brownian motion, in \mathbb{R} , characterized by independent Gaussian increments: $\mathbb{E}[dW_t] = 0$ and $\mathbb{E}[dW_s dW_t] = \delta(t - s)$.

In the absence of the additional feedback term involving the time-averaged position $\frac{1}{t} \int_0^t X_s ds$, Eq. (1) is the classical Ornstein–Uhlenbeck (OU) process, describing a Brownian agent moving in a parabolic potential well centered on the origin. As we will show, the inclusion of the empirical time-averaged position introduces a non-Markovian feedback that can give rise to unique dynamical behavior, effectively modifying the potential in which the particle evolves. This results in an *effective potential* whose minimum shifts along \mathbb{R} depending on the cumulative history of the process. We discuss this in more detail in Section II B.

Our objective is to analyze how this non-Markovian feedback influences the escape dynamics of X_t through a threshold $x_f > 0$, with a particular focus on the role of noise and memory. The feedback term can be expressed as

$$\bar{X}_t := \frac{1}{t} \int_0^t X_s ds \quad (2)$$

$$= \int_{\mathbb{R}} x \rho_t(x) dx, \quad \text{where} \quad (3)$$

$$\rho_t(x) = \frac{1}{t} \int_0^t \delta(X_s - x) ds \quad (4)$$

is the empirical occupation measure of the process. This measure captures the fraction of time the system has spent in the vicinity of each position x up to time t .

Although because its evolution depends on its entire history, the process $(X_t)_{t \geq 0}$ is non-Markovian, the joint two-dimensional process $(X_t, \bar{X}_t)_{t \geq 0} =: (Z_t)_{t \geq 0}$ is Markovian and satisfies:

$$\begin{cases} dX_t &= -X_t dt + \beta \bar{X}_t dt + \sqrt{\epsilon} dW_t \\ d\bar{X}_t &= \frac{X_t - \bar{X}_t}{t} dt. \end{cases} \quad (5)$$

Despite the fact that the process $(Z_t)_{t \geq 0}$ is time-inhomogeneous, the Markovian formulation (5) allows us to study the escape dynamics of the feedback OU process semi-analytically in the weak-noise regime, as shown in Section III C.

B. Mapping to Self-Interacting Diffusion Processes

The structure of the feedback embodied in Eqs. (2)–(4), allows the process $(X_t)_{t \geq 0}$ in Eq. (1) to be interpreted as a specific case of a one-dimensional self-interacting diffusion (SID). A general SID in \mathbb{R}^d is typically expressed as

$$dX_t = -\nabla V(X_t) dt - \frac{1}{t} \left(\int_0^t \nabla W(X_s, X_t) ds \right) dt + \sqrt{\epsilon} dW_t, \quad (6)$$

where $V(X_t)$ is a background potential and $W(X_s, X_t)$ is an interaction potential whose gradient is taken with respect to X_t . The interaction term describes how the current position is influenced by the history of past positions.

For the case of Eq. (1), the potentials in Eq. (6) take the form

$$V(X_t) = (1 - \beta) \frac{X_t^2}{2} \quad \text{and} \quad (7)$$

$$W(X_s, X_t) = W(X_t - X_s) = \beta \frac{(X_t - X_s)^2}{2}. \quad (8)$$

Therefore, a quadratic interaction potential W describes the attraction of the current position X_t to the past positions X_s , so that the general behavior of the process is determined by the combination of this interaction and the background potential V .

By rewriting Eq. (1), we can define an effective potential

$$\tilde{V}(X_t) = V(X_t) + \frac{1}{t} \int_0^t W(X_s, X_t) ds, \quad (9)$$

whose shape evolves according to the past trajectory of the process. For example, the minimum of this effective potential may shift to the left or right of the origin depending on whether the integral contribution in Eq. (9) is negative or positive, respectively.

Eqs. (7) and (8) make clear that for $\beta < 1$ ($\beta > 1$), the background potential remains quadratic and attractive (repulsive) around the origin. Although the process is still attracted to its past positions through the interaction potential W , the repulsive background potential drives escape towards infinity, which justifies the choice $\beta < 1$ described when we introduced Eq. (1).

More generally, Eq. (1) can be extended to incorporate alternative forms of feedback, such as

$$\bar{K}_t := t^{-\alpha} \int_0^t f(X_s) ds, \quad (10)$$

with $\alpha > 0$, which ensures a decaying contribution, with slower decay as α decreases, and f is an arbitrary function on \mathbb{R} . Although the methods developed here could be generalized to such circumstances, we focus on the simplest and most natural case: feedback via the empirical average position, corresponding to $\alpha = 1$ and $f(X_s) = X_s$. Importantly, this choice enables an exact mapping to SID processes. Alternative values of α , or more general time-dependent functions, would typically not allow this mapping and thus preclude comparison with well-established convergence properties of SIDs, which we discuss in Section IID.

C. Exact Results for the Deterministic Dynamics

Before analyzing the stochastic dynamics of the feedback OU process, we examine some essential features of the deterministic dynamics, obtained by setting $\epsilon = 0$ in Eqs. (1) or (5). This analysis provides insight into the behavior of the system and helps clarify the choice of the parameter range for β .

We set $\epsilon = 0$ in Eq. (5), which becomes the following first-order, time-inhomogeneous linear system of differential equations;

$$\dot{Z}_t = A_t(\beta)Z_t, \quad (11)$$

where $(\dot{})$ denotes the time derivative, and the time-dependent drift matrix is

$$A_t(\beta) = \begin{pmatrix} -1 & \beta \\ \frac{1}{t} & -\frac{1}{t} \end{pmatrix}. \quad (12)$$

For $\beta \in \mathbb{R} \setminus \{1\}$, the only fixed point of the system is the origin $(0, 0)$. However, when $\beta = 1$, all points satisfying $X = \bar{X}$ are fixed points.

The stability of the origin depends on both β and time as follows:

$\beta < 0$: The origin is stable, but exhibits a spiral-like behavior in the finite time window $[t_-, t_+]$ defined below.

$\beta \in [0, 1)$: The origin is a stable node.

$\beta > 1$: The origin becomes a saddle point, and an instability develops along a specific direction. At the bifurcation point $\beta = 1$, all points $X = \bar{X}$ are neutrally stable.

Due to the linearity of Eq. (11), stability is fully characterized by the eigenvalues of the 2×2 matrix $A_t(\beta)$, which are given by:

$$\lambda_t^\pm = \frac{-(1+t) \pm \sqrt{(1+t)^2 - 4t(1-\beta)}}{2t}. \quad (13)$$

For $\beta \in [0, 1)$, eigenvalues are both real and the square root term in Eq. (13) satisfies:

$$\sqrt{(1+t)^2 - 4t(1-\beta)} \leq 1+t, \quad (14)$$

implying that both eigenvalues λ_t^\pm are negative for all $t > 0$, and the origin is a stable node.

For $\beta < 0$, the discriminant in Eq. (13) can become negative, leading to complex eigenvalues. This occurs when $t \in [t_-, t_+]$, where

$$t_\pm = -(2\beta - 1) \pm 2\sqrt{\beta(\beta - 1)}. \quad (15)$$

Since the real parts of both eigenvalues remain negative, the origin remains stable, but the dynamics exhibit a spiral behaviour during this time interval.

For $\beta > 1$, eigenvalues are both real again and the situation is reversed: one eigenvalue $\lambda_t^- < 0$, while the other $\lambda_t^+ > 0$. An unstable direction thus emerges, associated with the eigenvector

$$u_t^+ = \begin{pmatrix} \frac{1}{2} \left[1 - t + \sqrt{(1+t)^2 - 4t(1-\beta)} \right] \\ 1 \end{pmatrix}. \quad (16)$$

Here, the fixed point at the origin becomes a saddle. When $\beta = 1$, the direction $X = \bar{X}$ is neutrally stable with $\lambda_t^+ = 0$. Thus, any small perturbation to $(0, 0)$ not orthogonal to u_0^+ will drive the system away from the fixed point, growing asymptotically along the direction of u_t^+ , with X and \bar{X} increasing proportionally, as in Eq. (16).

The following features of the deterministic dynamics have the following important implications for the stochastic system.

- (1) If one conditions on $X_T = x_f > 0$, then when $\beta > 1$ even a small perturbation due to noise will cause the process to escape the origin deterministically towards x_f . In such a regime, noise merely initiates the escape, but deterministic dynamics dominate the evolution.
- (2) The interesting regime is when $\beta < 1$. For $\beta \in [0, 1)$, the feedback in Eq. (1) is positive, so the most likely escape to $x_f > 0$ occurs through the accumulation of positive fluctuations. However, for $\beta < 0$, this intuitive picture breaks down: as positive fluctuations accumulate, the feedback becomes increasingly negative, pulling the process back toward the origin and making escape through x_f highly unlikely.

Therefore, two alternative escape mechanisms for the stochastic dynamics emerge:

- (3) (a) A one-stage mechanism, whereby large fluctuations are sufficient to overcome the negative feedback. This is an extremely rare event in the weak-noise limit. (b) A two-stage mechanism, whereby the stochastic process first accumulates negative fluctuations, generating a strong positive feedback, which then drives a “slingshot” escape to the right; $x_f > 0$.

These β -dependent qualitatively distinct escape pathways raise a natural question: in a symmetric domain $[-x_f, x_f]$, with $\beta \in [0, 1)$, is the agent more likely to escape to the right via the accumulation of positive fluctuations, or to the left by exploiting a slingshot mechanism? We return to these questions in Section IV.

In the next section (IID), we characterize the long-time behavior of general SIDs and feedback processes, which will serve as a useful reference for our analysis of finite-time escape dynamics.

D. Long-Time Behavior of the Feedback Ornstein–Uhlenbeck Processes

Having established in Section IIB that the feedback OU process in Eq. (1) belongs to the class of SIDs, we now draw on results from SID theory to understand the important asymptotic behavior. This will prove useful later, particularly in Sections IVB and IV C, when interpreting our results.

The long-time behavior of self-interacting processes, including random walks and diffusions, have been an active area of study in the probability theory community for the past two decades. Self-interacting random walks were first introduced by Norris et al. [48], in the discrete-time setting. Their continuous-time counterparts emerged as models for polymer growth in [49], and the *normalized* form considered here (as in Eq. (6)) was first introduced by Benaïm et al. [27]. While most early work focused on asymptotic properties, more recent studies [45, 50] have developed refinements of Kramers’ law for SIDs (see also [46, 47] for generalized overdamped Langevin systems). A recent contribution by one of us addresses large deviations for SIDs on a ring [43].

Convergence results for SIDs on compact spaces were developed in [27, 51–53], and later extended to open domains, such as on \mathbb{R}^d in [30, 54, 55], which is relevant for our feedback OU process. More recently, these results have been extended to systems with general additive noise [45, 50, 56]. Provided certain regularity conditions on the potentials are met and assuming confining potentials with at most polynomial growth, these results describe well the long-time behavior of the SID in Eq. (6), with potentials given by Eqs. (7) and (8), or equivalently the feedback OU process (1) for $\beta \in [0, 1)$.

Assuming stationary behavior at long times (as in [27, 43, 50]), one can formally derive the stationary occupation measure, or invariant density, ρ_{inv} of the general SID in Eq. (6) from the stationary Fokker–Planck equation (see [43]):

$$\rho_{\text{inv}}(x) = \frac{e^{-\frac{2}{\epsilon}(V(x) + \int_{\mathbb{R}^d} W(y,x)\rho_{\text{inv}}(y) dy)}}{Z}, \quad (17)$$

where Z is a normalization constant. The symmetry of the potential V in Eq. (7) is inherited by the invariant density ρ_{inv} [45, 50, 57], and in the case of the feedback OU process Eq. (1), Eq. (17) becomes

$$\rho_{\text{inv}}(x) = \sqrt{\frac{1}{\pi\epsilon}} e^{-\frac{x^2}{\epsilon}}, \quad (18)$$

which coincides with the stationary distribution of the standard OU process. In consequence, the memory feedback term in Eq. (2) converges in probability to

$$\bar{X}_t \xrightarrow{t \rightarrow \infty} 0. \quad (19)$$

Therefore, the classical OU process is recovered as the long-time limit of the feedback OU process. However, it is important to note that the convergence to this fixed point occurs *very-slowly*; slower than any algebraic rate. This has been shown in [45, 50, 55]: see Theorems 1.6 and 1.12 in [55], Theorem 2.7 in [50], and Theorem 2.10 and Propositions 2.11–2.12 in [45]. These long-time results serve as a valuable benchmark for understanding the finite-time dynamics studied in the remainder of this paper, where the memory feedback has a controlling influence.

We conclude this section by highlighting Theorem 2.13 from Aleksian et al. [45], which is relevant to our study. In the weak-noise limit $\epsilon \rightarrow 0$, they established a Kramers-type law for the escape probability of the agent in Eq. (6) through an open domain \mathcal{D} such that the boundary is $\partial\mathcal{D} \subset \mathbb{R}^d$. They assumed the potentials V and W are uniformly convex with at most polynomial growth and V such that $\lim_{|x| \rightarrow \infty} |\nabla V(x)|^2/V(x) = +\infty$. This last condition does not hold for the V in Eq. (7). The escape probability distribution can be expressed as:

$$\mathbb{P}(X_\tau \in \partial\mathcal{D}) \approx e^{-\frac{2}{\epsilon} \inf_{x \in \partial\mathcal{D}} H(x)}, \quad (20)$$

where

$$H(x) := V(x) + W(x - m) - V(m), \quad (21)$$

where the first time the process exits the domain \mathcal{D} is $\tau := \inf\{t \geq 0 : X_t \notin \mathcal{D}\}$, and m is the point at which ρ_{inv} attains its maximum. For the feedback OU process in Eq. (1), we have $m = 0$ and we typically consider a single escape boundary $\partial\mathcal{D} = \{x_f\}$. Therefore, the rate function becomes:

$$H(x_f) = x_f^2. \quad (22)$$

We note that this result was derived under the further assumption that the empirical occupation measure stabilizes prior to escape. As we show in Section III A using a weak-noise large deviation approach, our analysis does not require this assumption, which leads to a strong dependence of the escape dynamics on the value of $\beta \in [0, 1)$, as we will explore in detail.

Finally, we emphasize that Eq. (20) characterizes the probability of escape *at a given time*, rather than the mean escape time. As such, it does not constitute an Arrhenius-type law, which would describe the expected time to escape (this is also noted in the Appendix of [45]). The quantification of an Arrhenius law for the feedback OU process, and its relation to the underlying large deviation principles, is one of the main results of our work.

III. ESCAPE DYNAMICS AND WEAK-NOISE LARGE DEVIATIONS

Given the Markovian structure of the dynamics in Eq. (5), the associated time-dependent infinitesimal generator takes the form:

$$L_t = A_t(\beta)z \cdot \nabla + \frac{\epsilon}{2} \frac{\partial^2}{\partial x^2}, \quad (23)$$

where $z := (x, \bar{x})$ and ∇ denotes the gradient with respect to the variables (x, \bar{x}) . This generator can be used to extract information on the escape dynamics, in particular: (i) the escape time distribution $f_T(x_f)$, and (ii) the mean escape time \bar{T} , defined as the first moment of $f_T(x_f)$.

The escape time distribution is given by

$$f_T(x_f) := -\frac{\partial P_T(x_f)}{\partial T}, \quad (24)$$

where

$$P_T(x_f) = \int P_0(x) P(X_T = x_f | X_0 = x) dx, \quad (25)$$

is the probability density of the process $(X_t)_{t \geq 0}$ evaluated at time $t = T$ and position $x = x_f$, given $P_0(x_0)$, the initial, and $P(X_T = x_f | X_0 = x_0)$ the transition probability density of the process. Importantly, we note that $P(X_T = x)$ is shorthand for the probability that X_T lies in a small interval $[x, x + dx)$, so that the probability density satisfies $\mathbb{P}_T(x_f) = P_T(x_f) dx$, where $\mathbb{P}_T(x_f)$ is the probability distribution.

By initializing the process at the origin, the probability density $P_T(x)$ satisfies the following Fokker–Planck boundary value problem;

$$\frac{\partial P_T(x)}{\partial T} = L_T^\dagger P_T(x), \quad \text{with} \quad P_0(x) = \delta(x) \quad \text{and} \quad P_T(x_f) = 0, \quad (26)$$

where L_T^\dagger denotes the adjoint of the generator L_T in Eq. (23). Additionally, the mean escape time \bar{T} satisfies the following boundary value problem [58]:

$$\begin{cases} (L_T + \frac{\partial L_T}{\partial T}) \bar{T} = -1, & \text{for } x < x_f, \\ \bar{T} = 0, & \text{for } x = x_f. \end{cases} \quad (27)$$

It is important to note that the infinitesimal generator L_T is explicitly time-dependent due to the drift term, and the diffusion is degenerate, since no noise acts directly on the dynamics of \bar{X}_t . For these reasons, exact analytical solutions to Eqs. (26) and (27) are generally not available.

However, asymptotic approaches are possible. For instance, approximate analytical solutions for both the autonomous and non-autonomous one-dimensional Ornstein–Uhlenbeck processes and for stochastic resonance have recently been obtained using matched asymptotic expansions [59–62]. While this approach could in principle be extended to the two-dimensional setting considered here, identifying the appropriate boundary layers in two dimensions is highly non-trivial and would require a separate in-depth study.

Instead, here we use the framework of weak-noise large deviation theory to derive asymptotic results for the escape dynamics of the feedback OU process. In the weak-noise regime, we can analyze the asymptotic behavior of the probability $P_T(x_f)$ by solving an effective approximation of Eq. (26), that is the associated Hamilton–Jacobi equation.

In Section III A, we briefly review the general weak-noise large deviation framework for Markov processes—see [63–65] for more comprehensive treatments. We then illustrate how this framework can be used to extract relevant information about escape dynamics and apply it to both the standard OU process (Section III B) and the feedback OU process (Section III C).

A. Weak-Noise Large Deviations

We introduce the weak-noise large deviation framework by considering a d -dimensional Markov process $(Z_t)_{t \geq 0}$ governed by the stochastic differential equation,

$$dZ_t = F_t(Z_t) dt + \sqrt{\epsilon} \sigma dW_t, \quad (28)$$

where F_t is a (possibly time-dependent) d -dimensional drift vector field, $\sigma \in \mathbb{R}^{d \times d}$ is a constant noise matrix, $D = \sigma^T \sigma$ is the noise covariance (diffusion) matrix, and W_t is a d -dimensional Brownian motion. For simplicity, we assume additive noise, i.e., σ does not depend on position, and we consider a pointwise initial condition $Z_0 = z_0$.

Similarly to Section III, we are interested in the asymptotic behavior of the probability density,

$$P_t(z) = \int P_0(z_0) P(Z_t = z | Z_0 = z_0) dz_0, \quad (29)$$

which satisfies the following Fokker–Planck equation,

$$\partial_t P_t(z) = -\nabla \cdot (F_t(z) P_t(z)) + \frac{\epsilon}{2} \nabla \cdot (D \nabla P_t(z)), \quad (30)$$

with initial condition $P_0(z) = \delta(z - z_0)$.

Now, by assuming an exponential scaling in ϵ and making the following change of variable,

$$P_t(z) = \exp[-\epsilon^{-1}S_t(z)] , \quad (31)$$

taking the weak-noise limit, $\epsilon \rightarrow 0$, and retaining terms up to order $O(\epsilon^{-1})$, gives the following Hamilton–Jacobi equation [65]:

$$-\partial_t S_t(z) = H_t(z, \nabla S_t(z)) . \quad (32)$$

Here, the time-dependent Hamiltonian is given by

$$H_t(z, p) = \frac{1}{2} p \cdot D p + F_t(z) \cdot p , \quad (33)$$

where p denotes a vector of adjoint variables, or momentum coordinates. The approximation introduced through the change of variable (31) with $\epsilon \ll 1$ is commonly referred to as the WKBJ (after Wentzel, Kramers, Brillouin and Jeffreys) ansatz in many areas of physics, including stochastic processes [59, 66, 67].

The Hamilton–Jacobi equation (32) is a first-order partial differential equation whose solution can be obtained from the characteristic curves of the associated Hamiltonian dynamics, which are

$$\dot{z}_t = \nabla_p H_t(z, p) \quad \text{and} \quad \dot{p}_t = -\nabla_z H_t(z, p) , \quad (34)$$

subject to appropriate boundary conditions.

By integrating along these characteristic trajectories—often referred to as *instantons* in the large deviation literature [65, 66]—the action functional in Eq. (32) takes the following form;

$$S_t(z) = \int_0^t [p \cdot \dot{z} - H_t(z, p)] dt + S_0(z_0) . \quad (35)$$

This expression reflects the fact that the action is the generating function of a canonical transformation, linking the first-order PDE (32) with the second-order Hamiltonian dynamics of Eq. (34) [68, 69].

In the weak-noise regime, the action so obtained represents the dominant contribution to the probability density function $P_t(z)$ in Eq. (31), wherein, with a slight abuse of notation, we denote both the full action and its leading-order contribution at $O(\epsilon^{-1})$ with the same symbol. This action determines the asymptotic behavior in ϵ^{-1} of the probability of finding the process at z_f for the first time T , as in Eq. (25), viz.

$$P_T(z_f) \approx \exp[-\epsilon^{-1}S_T(z_f)] . \quad (36)$$

Moreover, upon taking the time derivative of Eq. (36), we find that in the weak-noise limit the escape time distribution in Eq. (24) is also approximated by $P_T(z_f)$ of Eq. (36).

The optimal trajectory z_t is that which minimizes the action, which defines the instanton. Thus, the instanton corresponds to the most likely path connecting the initial point z_0 to the final point $z_T = z_f$ as $\epsilon \rightarrow 0$, thereby providing the dominant path through which the system escapes to z_f at time T .

By integrating over time, Eq. (36) leads to the Kramers-type, or Arrhenius-type, formula as

$$P(z_f) \approx \exp[-\epsilon^{-1}U(z_f)] , \quad (37)$$

where

$$U(z_f) := \inf_{T \geq 0} S_T(z_f) \quad (38)$$

is the quasi-potential, or the large deviation rate function. We interpret $U(z_f)$ as an effective energy barrier that the system must overcome to reach z_f , and it governs the leading-order behavior of the escape probability. Additionally, the optimal escape time can be determined as

$$\tau(z_f) = \operatorname{arginf}_{T \geq 0} S_T(z_f) . \quad (39)$$

We note that in general this optimal escape time $\tau(z_f)$ is not equivalent to the mean escape time (approximated by the inverse Kramers rate), which corresponds to the solution of the backward equation (27). Although the two quantities are related, they have distinct interpretations. The optimal escape time is based on the idea that the system drifts toward z_f as slowly as possible to minimize the action. However, real escape events are noise induced and occur asymptotically on a finite timescale given by the inverse Kramers rate in Eq. (37).

B. The Weak-Noise Regime of the Ornstein–Uhlenbeck Process

As noted above, a canonical analytically tractable stochastic process in statistical physics is the Ornstein–Uhlenbeck process, which is obtained by removing the feedback term, $\frac{1}{t} \int_0^t X_s ds$, from Eq. (1). The transition probability density function is a Gaussian that can be computed explicitly by solving the Fokker–Planck equation

$$\partial_t P_t(x) = L^\dagger P_t(x), \quad (40)$$

with initial condition $P_0(x) = \delta(x)$, where L is the infinitesimal Markov generator given by

$$L = -x \frac{d}{dx} + \frac{\epsilon}{2} \frac{d^2}{dx^2}. \quad (41)$$

Equation (40) can be solved using Fourier transform or heat kernel methods giving the transition probability density as

$$P_t(x) = \sqrt{\frac{1}{\pi\epsilon(1-e^{-2t})}} \exp\left[-\frac{1}{\epsilon} \frac{x^2}{(1-e^{-2t})}\right], \quad (42)$$

which is the probability of finding the process at position x at time t .

Because Eq. (42) takes a large deviation form, we identify the action S_T^{OU} in Eq. (36) as

$$S_T^{\text{OU}}(x_f) := \frac{x_f^2}{1-e^{-2T}}. \quad (43)$$

As discussed in Section III A, this gives an asymptotic characterization of the probability of finding the OU process at x_f for the first time T ; it provides the leading-order asymptotic form of the escape time distribution in Eq. (24).

By solving Eqs. (34) for the Hamiltonian in Eq. (33), which in this case is $H(x, p) = \frac{1}{2}p^2 - px$, we obtain the instanton equation

$$x_t^{\text{OU}} = x_f \frac{\sinh t}{\sinh T}, \quad (44)$$

which gives the most probable path from $x_0^{\text{OU}} = 0$ to $x_T^{\text{OU}} = x_f$.

Integrating Eq. (42) in time yields the probability of being at x as an implicit function of time;

$$P(x) = \frac{|x|}{\sqrt{\pi\epsilon}} \int_{\frac{|x|}{\sqrt{\epsilon}}}^{\infty} \frac{e^{-t^2}}{t^2 - \frac{|x|}{\sqrt{\epsilon}}} dt, \quad (45)$$

and its leading-order behavior in ϵ^{-1} , which can also be obtained from Eq. (38), is given by the following quasi-potential

$$U^{\text{OU}}(x_f) = x_f^2, \quad (46)$$

which is quadratic in the final position as expected. Moreover, we note that the quasi-potential for the OU process coincides with $H(x_f)$ in Eq. (22).

Finally, the escape time of the process generally depends on the noise intensity ϵ . Although the mean escape time is finite and given by the inverse Kramers rate, in the weak-noise limit inspection of Eq. (39) shows that the optimal escape time diverges; $\tau \rightarrow \infty$. Therefore, the weak-noise OU process tends to remain near the bottom of the potential well for as long as possible in order to minimize the action, eventually escaping the quadratic trap through a single large fluctuation.

C. The Weak-Noise Regime of Feedback Ornstein–Uhlenbeck Processes

We now turn our attention to the feedback OU process. Rather than analyzing the non-Markovian process X_t defined by Eq. (1), we consider the two-dimensional Markovian process $Z_t = (X_t, \bar{X}_t)$ defined by Eq. (5). The dynamics is governed by Eq. (28), with a deterministic time-dependent drift given by

$$F_t(Z_t) = A_t(\beta)Z_t, \quad (47)$$

and a noise matrix

$$\sigma = D = \begin{pmatrix} 1 & 0 \\ 0 & 0 \end{pmatrix}, \quad (48)$$

showing that noise acts only on the X_t component. (We discuss the consequences of the structure of the noise matrix below.) We consider the initial condition $Z_0 = (X_0, \bar{X}_0) = (0, 0)$, which also regularizes the singularity at $t = 0$, and we aim to study the escape dynamics through $x_f > 0$.

The time-dependent Hamiltonian is given by

$$H_t(z, p) = \frac{p_x^2}{2} - (x - \beta\bar{x})p_x + \frac{(x - \bar{x})}{t}p_{\bar{x}}, \quad (49)$$

where $z = (x, \bar{x})$ and $p = (p_x, p_{\bar{x}})$. The solutions to the Hamilton–Jacobi equation (32) are obtained by solving the associated Hamilton equations (34) and are:

$$\begin{cases} \dot{x} = p_x - x + \beta\bar{x} \\ \dot{\bar{x}} = \frac{x - \bar{x}}{t} \\ \dot{p}_x = p_x - \frac{p_{\bar{x}}}{t} \\ \dot{p}_{\bar{x}} = -\beta p_x + \frac{p_{\bar{x}}}{t} \end{cases} \quad \begin{cases} x_0 = 0 \\ \bar{x}_0 = 0 \\ p_{x,T} = \lambda \\ p_{\bar{x},T} = 0 \end{cases}. \quad (50)$$

Here, λ is a parameter implicitly determined by the final condition $x_T = x_f$ through the Hamiltonian dynamics. As we highlight in the derivation below, it is more convenient to impose final conditions on the adjoint variables rather than initial conditions on the adjoint variables or final conditions on the coordinate variables. We also refer the reader to Section 2.4.1 of [70] for an explanation of how to transform final conditions on position variables into final conditions on adjoint variables within a Lagrangian framework.

Starting from Eqs. (50), we derive a simplified differential equation the solution to which gives the instanton. Importantly, the adjoint equations are decoupled from the coordinate variables, which allows us to solve them independently and substitute their solution into the coordinate equations.

We begin with the equation for \dot{p}_x . To simplify the analysis, we assume that $p_{\bar{x}}$ does not explicitly depend on p_x . Although this assumption may conflict with the last equation in (50), we adopt it here as an *ansatz* and will post hoc verify its validity. Applying separation of variables and variation of constants, we obtain the following

$$p_{x,t} = \lambda e^{-(T-t)} - \int_t^T \frac{p_{\bar{x},s} e^{(t-s)}}{s} ds, \quad (51)$$

where the constant of integration is fixed by the boundary condition $p_{x,T} = \lambda$. Note that because the momentum grows exponentially in time, this is why it is preferable to impose a final rather than an initial condition on the momentum, which naturally constrains the unbounded growth of the solution.

Substituting Eq. (51) into the equation for $p_{\bar{x}}$ and differentiating both sides with respect to t , we obtain the following second-order differential equation:

$$\ddot{p}_{\bar{x}} = \dot{p}_{\bar{x}} \left(1 + \frac{1}{t}\right) + \frac{p_{\bar{x}}}{t} \left(\beta - 1 - \frac{1}{t}\right). \quad (52)$$

This equation must be solved subject to the boundary conditions that $p_{\bar{x},T} = 0$, as in Eq. (50), and $\dot{p}_{\bar{x},T} = -\beta\lambda$, which follows directly from the evolution equation for $p_{\bar{x}}$.

The general solution of Eq. (52) is given in terms of special functions as

$$p_{\bar{x},t} = t (c_1 \text{HypU}[\beta, 1, t] + c_2 \text{LagL}[-\beta, t]), \quad (53)$$

where c_1 and c_2 are constants, the first term on the right-hand side is the Tricomi confluent hypergeometric function,

$$\text{HypU}[a, b, t] = \frac{1}{\Gamma(a)} \int_0^\infty e^{-st} s^{a-1} (1+s)^{b-a-1} ds, \quad (54)$$

and $\text{LagL}[n, t]$ is the Laguerre polynomial, defined as the solution of Laguerre’s differential equation;

$$ty'' + (1-t)y' + ny = 0, \quad (55)$$

where n is a non-negative integer. It can be shown that Eq. (53) satisfies $p_{\bar{x},0} = 0$, ensuring regularity in the limit $t \rightarrow 0$ in Eq. (50). The same regularity is obtained by formally considering the asymptotic limit of $\beta \rightarrow 0$ or for $t \ll 1$ or both. In both cases, $\dot{p}_{\bar{x}} = -\beta p_x + \frac{p_{\bar{x}}}{t}$ becomes $\dot{p}_{\bar{x}} = \frac{p_{\bar{x}}}{t}$, so that $p_{\bar{x}} = Ct$ and hence $\dot{p}_x = p_x - C$, which in turn shows the validity of the ansatz considered.

Imposing the two boundary conditions above determines the constants in Eq. (53) as

$$c_1 = \frac{\beta\lambda \text{LagL}[-\beta, T]}{\beta T \text{HypU}[1 + \beta, 2, T] \text{LagL}[-\beta, T] - T \text{HypU}[\beta, 1, T] \text{LagL}[-1 - \beta, 1, T]} \quad \text{and} \quad (56)$$

$$c_2 = -\frac{\beta\lambda \text{HypU}[\beta, 1, T]}{\beta T \text{HypU}[1 + \beta, 2, T] \text{LagL}[-\beta, T] - T \text{HypU}[\beta, 1, T] \text{LagL}[-1 - \beta, 1, T]}. \quad (57)$$

This completes the solution Eq. (53) of Eq. (52), thereby providing an explicit expression for $p_{x,t}$ in Eq. (51).

Differentiating the first equation in (50), substituting the expression for $\dot{\bar{x}}$, and using the first equation again to eliminate \bar{x} , we obtain the following second-order differential equation for x_t ,

$$\ddot{x} = \dot{p}_x - \left(1 + \frac{1}{t}\right) \dot{x} + \frac{p_x}{t} + (\beta - 1) \frac{x}{t}, \quad (58)$$

which can be rewritten, using Eq. (51), as

$$\ddot{x} = \left(1 + \frac{1}{t}\right) (p_x - \dot{x}) - \frac{1}{t} (p_{\bar{x}} - (\beta - 1)x). \quad (59)$$

This equation must be solved using $p_{x,t}$ from Eq. (51), $p_{\bar{x},t}$ from Eq. (53), and boundary conditions $x_0 = 0$ and $\dot{x}_0 = p_{x,0}$. The latter condition follows directly from the initial condition $\bar{x}_0 = 0$ and the Hamiltonian equation for \dot{x} . The dynamics of \bar{x}_t can then be recovered by inverting the equation for \dot{x} once the solution to Eq. (59) is known.

In summary, we have reduced the full system Eqs. (50) to a single second-order differential equation (59), whose solution provides the instanton x_t connecting $x_0 = 0$ to $x_T = x_f$, which indirectly determines \bar{x}_t . The solution to Eq. (59) must be computed numerically. We compare the instantons of the OU process and the feedback OU process in Figs. 1 and 2 of Section IV A.

Once the instanton solution is obtained, we can compute the action using Eq. (35), with $p = (p_x, p_{\bar{x}})$, the Hamiltonian (49), and $S_0(x_0, \bar{x}_0) = 0$, since the process starts at the minimum of the potentials V and W given by Eqs. (7) and (8). The weak-noise approximation of the escape probability through x_f is then given by Eq. (37), with:

$$z_f = (x_f, \bar{x}_f), \quad (60)$$

where x_f is prescribed, and \bar{x}_f is determined from the solution of Hamilton's equations. The quasi-potential and optimal escape time are finally obtained using Eqs. (38) and (39), respectively.

We conclude this section by highlighting the following. A natural approach to deriving the instanton equation would have been to consider the Lagrangian $L(z, \dot{z}) = \langle \dot{z} - F_t(z), D^{-1}(\dot{z} - F_t(z)) \rangle / 2$, where angle brackets denote the Euclidean scalar product. This dual Lagrangian derivation would have ensured that we would have to grapple with consequences of the singular nature of the matrix D . Indeed, the kernel of D is one-dimensional and may encode important information about the dynamics. For instance, using the Moore–Penrose inverse (pseudo-inverse), one would obtain an equation of the form $\ddot{x} = -(1 + t^{-1})\dot{x} + t^{-1}(\beta - 1)x$, the solution of which is the instanton. This equation for \ddot{x} , in contrast to Eq. (59), entirely misses the contribution of the adjoint dynamics. Thus, in such a formulation, it would be necessary to supplement the Euler–Lagrange equations with an additional kernel-dependent term, the analysis of which would require alternative methods. On the contrary, within the Hamiltonian framework no such issue arises: the degeneracy of D is not a problem and the adjoint dynamics are fully incorporated into the solution.

IV. NUMERICAL RESULTS AND DISCUSSION

A. Instanton Dynamics

We now compare and contrast the classical and feedback OU processes allowing us to characterize the physical mechanisms responsible for escape. In particular, we present our results on the instanton dynamics leading the feedback OU process to escape through $x_f > 0$, and compare them with the classical OU case.

To solve Eq. (59) numerically we use the `solve_ivp` solver from the `scipy.integrate` Python package, employing RK45, which corresponds to the explicit fourth order Runge–Kutta method of integration. In Fig. 1 we compare the numerical solution for the instanton x_t , obtained from the analytical approximation of Eq. (59), and the memory component \bar{x}_t , with simulations for three representative cases: $\beta < 0$ in Fig. 1(a), $\beta = 0$ (OU process) in Fig. 1(b), and $\beta > 0$ in Fig. 1(c). Clearly, the average behavior of sample-path simulations conducted at finite but small noise ϵ compares well with the instanton x_t , thereby supporting the ansatz considered and, more generally, our analytical derivation of Eq. (59).

Firstly, the case $\beta = 0$ shown Fig. 1(b) exhibits the classical OU instanton x_t^{OU} given by Eq. (44). For completeness, we also show the memory \bar{x}_t , defined in Eq. (2), which does not influence the dynamics in this case. As expected, the classical OU instanton corresponds to a monotonic exponential approach to x_f , as discussed in Section III B.

Secondly, Fig. 1 reveals qualitatively distinct escape mechanisms for negative and positive values of β , although both resemble the classical OU escape at late times.

For $\beta < 0$, Fig. 1(a) shows that since it is detrimental to accumulate positive fluctuations toward x_f , the process instead accumulates fluctuations in the opposite direction. Because $\beta < 0$, this effectively moves the

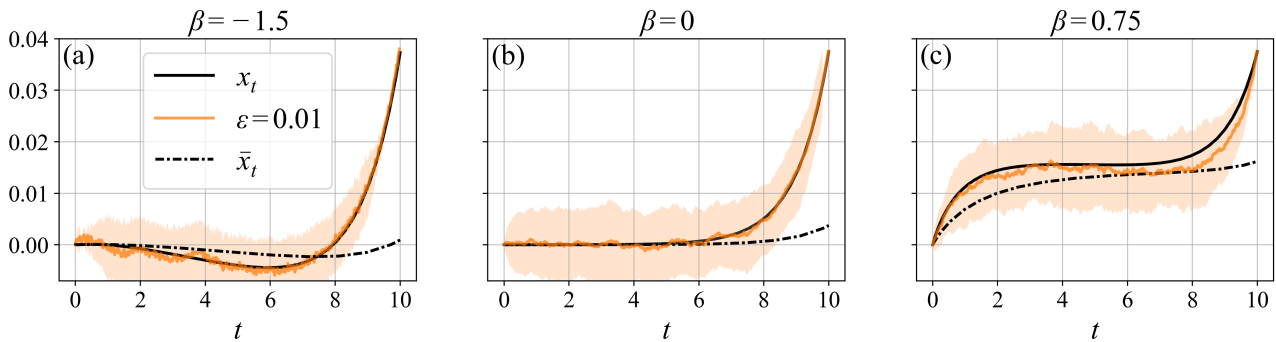


FIG. 1: Comparison between the instanton x_t solving Eq. (59) for $T = 10$ and numerical simulations of the feedback OU process governed by Eqs. (5), for three values of the feedback parameter: $\beta < 0$ (a), $\beta = 0$ (b), and $\beta > 0$ (c). In the small-noise regime $\varepsilon = 0.01$, the average simulated trajectory (solid orange line), computed over 10^7 realizations and post-selected on reaching $x_f = 0.0375$ at time $T = 10$, closely follows the instanton. The shaded area shows one standard deviation around the average. The corresponding memory trajectory \bar{x}_t , obtained by inverting the equation for \dot{x} in Eq. (50), is also shown. These results support the accuracy of the analytical approximation.

potential minimum toward x_f , storing a form of ‘potential energy’ that is then released through a monotonic exponential approach to x_f . We refer to this behavior as the ‘slingshot’ effect.

For $\beta > 0$, Fig. 1(c) shows that the process escapes optimally by initially accumulating small fluctuations toward x_f , which are stored in the memory \bar{x}_t , effectively shifting the minimum of the potential closer to x_f . As time progresses, the memory feedback becomes increasingly rigid due to averaging, which leads to a plateau in the intermediate time regime. However, since the effective potential minimum moves closer to x_f , escape becomes less costly in terms of the action (see Fig. 3) and we see the final exponential rise, again akin to the late time behavior of the classical OU case in Fig. 1(b).

As previously noted, for simplicity we restrict our analysis to the case with $x_f > 0$, but note that the case $x_f < 0$ can be treated analogously. Indeed, as shown in Fig. 2, changing the sign of x_f simply reflects the instanton trajectory, leaving the qualitative dynamics unchanged.

Having described the escape mechanisms of the feedback OU process, next we analyze the action function $S_T(z_f)$ in order to assess the likelihood of these mechanisms.

B. Time-Dependent Action

As defined in Eq. (35), the action $S_T(z_f)$ depends both on the escape point z_f in Eq. (60) and on the escape time T . Moreover, as shown in Eq. (36), the action determines the probability of finding the process at z_f for the first time T . In Fig. 3, we collect a series of plots illustrating the important behavior of this action.

In Fig. 3(a), we plot the action at a fixed escape point $x_f = 0.3$ as a function of time T , for five values of β . When $\beta < 0$ ($\beta > 0$) the action lies above (below) the analytical action S_T^{OU} of the classical OU process given in Eq. (43) and the black dashed line for $\beta = 0$. This implies that, for a given x_f , the finite-time slingshot mechanism employed by the feedback OU process with $\beta < 0$ is less probable than the accumulation of positive fluctuations occurring for $\beta > 0$.

When β is sufficiently negative, Fig. 3(a) shows the emergence of local and global minima, with the local

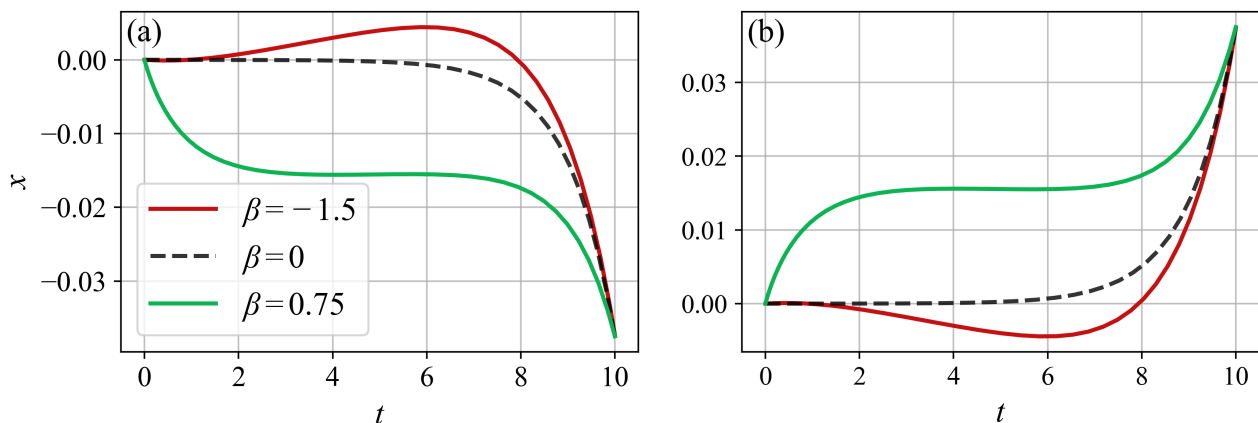


FIG. 2: Instanton x_t solutions of Eq. (59) for $T = 10$ and for the values of β in Fig. 1, plotted for a negative (a) and a positive (b) escape point x_f . Changing the sign of x_f corresponds to mirroring the instanton trajectories, thus fully characterizing the dynamics.

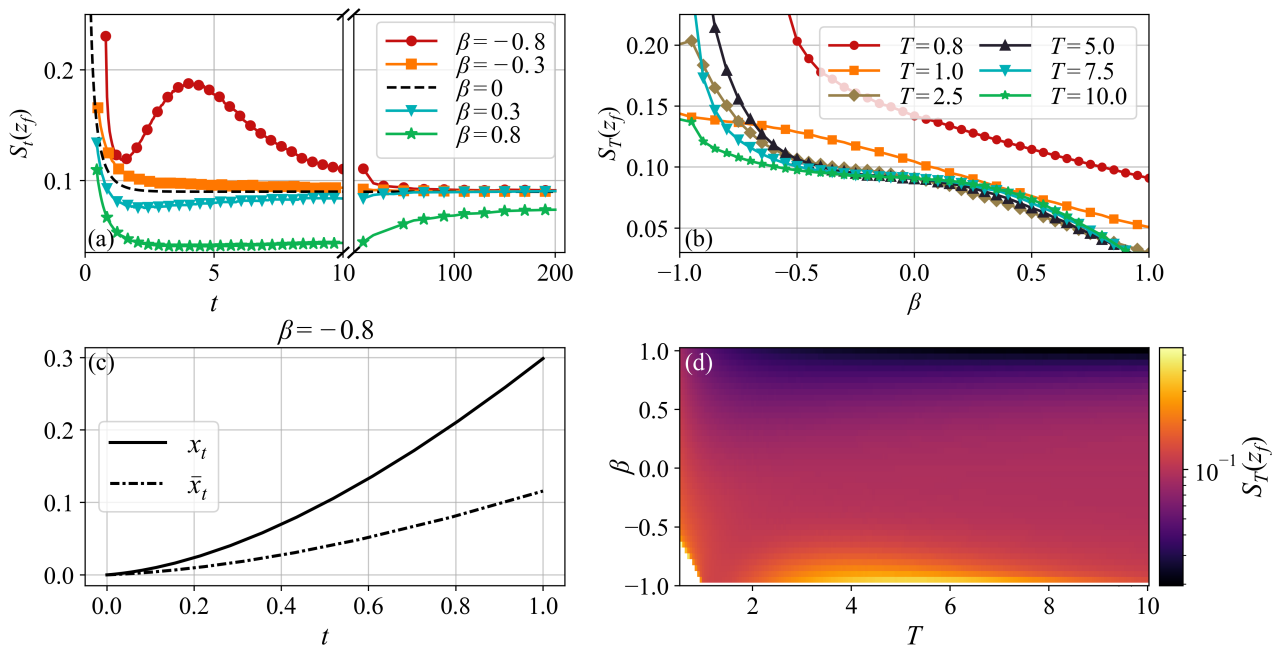


FIG. 3: (a) The action $S_T(z_f)$ (Eq. 35) as a function of time T , at a fixed $x_f = 0.3$, for several values of β . The classical OU action is the black dashed line ($\beta = 0$), with the feedback OU process curves above ($\beta < 0$) and below ($\beta > 0$). (b) The action plotted as a function of β , at fixed $x_f = 0.3$, for several values of T . (c) The instanton x_t and memory \bar{x}_t for $\beta = -0.8$ and $T = 1.0$, showing nearly ballistic dynamics associated with the local minimum in (a) and the non-monotonic time behavior in (b). (d) A heatmap of the action plotted as a function of escape time T and feedback parameter β , at fixed $x_f = 0.3$. The white regions indicate numerical failure in solving Eq. (59).

minimum occurring at short times and creating a sub-optimal time window for escape dynamics. Indeed, solving Hamilton's equations for this time and $x_f = 0.3$ reveals that the instanton dynamics is nearly ballistic, as seen in Fig. 3(c). However, as $\beta \rightarrow 0^-$ the sigmoidal structure, and hence the short-time local minimum, disappears as the global minimum is driven towards $T \rightarrow \infty$, as seen by the convergence of the colored curves towards the OU action from above. Thus, at large times, all escape mechanisms asymptote to the standard OU dynamics, confirming the theoretical results on the long-time behavior of self-interacting diffusions discussed in Section IID.

In contrast, when $\beta > 0$ the global minimum of the action moves from $T \rightarrow \infty$ to a finite time, the value of which decreases as β decreases. Therefore, accumulating and storing positive fluctuations via memory feedback is always more favorable than escaping through classical OU dynamics. This shift in the global minimum significantly influences the computation of the quasi-potential and optimal escape time, as discussed in Section IV C.

As seen in Fig. 3(b), for $\beta = 0$, classical OU escape dynamics are more probable as T increases, since the action decreases and approaches $\lim_{T \rightarrow \infty} S_T^{\text{OU}}(x_f)$. This behavior continues for a range of negative β until local minimum identified in Fig. 3(a) becomes influential, as reflected in the $T = 1.0$ curve which crosses the others and disrupts the monotonicity of the action with escape time. Thus, there is a threshold value $\beta \equiv \beta_c(x_f)$ such that for $\beta < \beta_c(x_f)$ ($\beta > \beta_c(x_f)$) the ballistic mechanism is more probable (less probable) than the slingshot mechanism. We numerically estimate $\beta_c(x_f) \approx -0.35$, a value that remains approximately constant over the range $x_f \in [-0.45, 0.45]$, where numerics is reliable.

A unified means of visualizing the information in Figs. 3(a) and (b) is obtained by constructing a heatmap of the action as a function of β and escape time T , at fixed $x_f = 0.3$, as shown in Fig. 3(d). Here we see that across all times the escape dynamics for $\beta < 0$, be they ballistic or slingshot, are less probable than for $\beta > 0$, where the accumulation of positive fluctuations dominates.

Similarly, in Fig. 4 we plot heatmaps of the action as a function of T and escape point x_f , for three fixed values of the feedback parameter β . Firstly, for all values of β the figures show that escaping through boundary points farther from the origin is unlikely, and least likely for $\beta < 0$. Secondly, the non-monotonicity discussed above is clearly seen in the patterns here, most notably for $\beta = -0.5$ in Fig. 4(a), where escape is less likely for $T = 5.0$ than for shorter or longer times. This reflects the local minimum in the action seen in Fig. 3(a) for $\beta < \beta_c(x_f)$, where short-time ballistic escape becomes the dominant mechanism.

In Section IV C, we turn to the time-independent properties of the escape dynamics, captured by the quasi-potential in Eq. (38). Additionally, we examine the Kramers escape rate and the optimal escape time introduced in Eq. (39).

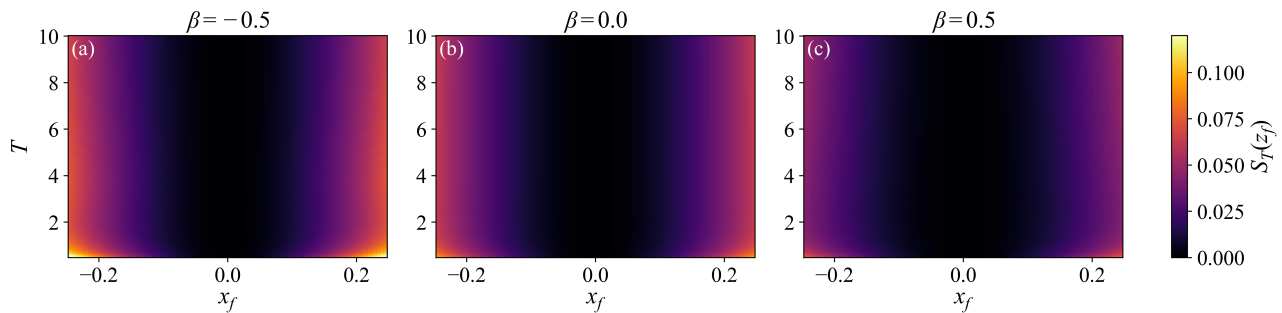


FIG. 4: Heatmaps of the action $S_T(z_f)$ as a function of x_f and T for three feedback parameters: $\beta = -0.5$ (a), $\beta = 0$ (b), and $\beta = 0.5$ (c).

C. Quasi-Potential and Optimal Escape Time

The quasi-potential $U(z_f)$ is the large deviation rate function governing the probability of finding the process at a point x_f in the small-noise limit $\epsilon \rightarrow 0$. It characterizes the effective ‘energy barrier’ that the process must overcome to escape through x_f . The larger the quasi-potential, the greater the barrier required for escape and the longer the mean escape time, which is approximated by the inverse of the probability in the Kramers rate formula in Eq. (38).

Fig. 5(a) shows $U(z_f)$ as a function of the escape point x_f for five values of β straddling the origin. Clearly, for $\beta > 0$ the quasi-potential lies below the $\beta = 0$ black dashed line corresponding to the OU result $U^{\text{OU}}(x_f) = x_f^2$ given in Eq. (46). This is a consequence of the global minimum of the action $S_T(z_f)$ occurring at finite time shown in Fig. 3(a). Thus, the most likely mechanism of reaching a given escape point x_f must have $\beta > 0$, and involves the accumulation of positive fluctuations in the memory. Moreover, as β increases, this mechanism becomes more likely.

Importantly, this behavior is significantly different from the scenario in which the empirical occupation measure stabilizes before escape, as discussed at the end of Section IID and reflected in the β -independent rate function in Eq. (22). We argue that this difference arises because the quasi-potential in Eq. (38), and shown in Fig. 5(a), is the infimum of the action, rather than its value in the infinite-time limit, which would be a sufficient condition for the stabilization of the occupation measure.

As expected, the quasipotential coincides with the OU result when $\beta < 0$, since the action S_T reaches a global minimum as $T \rightarrow \infty$, as discussed in Fig. 3.

In Fig. 5(b), we plot the quasi-potential as a function of β for five escape points x_f . The plateaus for $\beta < 0$ correspond to the OU value of Eq. (46). For $\beta > 0$, $U(z_f)$ decreases monotonically with β , reflecting the shift of the global minimum of the action to finite times. This reduction in the quasi-potential effectively lowers the escape barrier, thereby accelerating escape dynamics by reducing the mean escape time, which is approximated by taking the inverse of the Kramers rate in Eq. (37).

As previously, a heatmap perspective combines the behavior in a single figure, in this case the quasi-potential as a function of both β and x_f , as shown in Fig. 5(c). Key here is the enhanced escape through a fixed x_f with increasing β .

In summary, Fig. 5 demonstrates that, rather than classical OU dynamics or slingshot effects, memory-accumulated positive fluctuations towards the target is the most likely mechanism underlying the escape process through x_f . The transition between classical OU escape and that due to memory-accumulated positive fluctuations is delineated by $\beta = 0$.

Finally, in Fig. 6 we plot the optimal escape time τ as a function of β for three points x_f . This provides further evidence that the global minimum of the action S_T shifts from infinite time for $\beta \leq 0$ (with the proviso of the cut off at $T = 10$) to a finite time for $\beta \in (0, 1)$. Near $\beta = 0$ the transition appears abrupt, however, further investigation is needed to fully characterize the nature of this transition. The emergence of a finite optimal escape time for $\beta > 0$ reflects the role that feedback plays in accelerating the escape dynamics through memory-accumulated fluctuations.

Furthermore, for all x_f , the optimal escape time initially decreases with β , reaches a minimum, and then grows again for larger β , eventually reaching the numerical cutoff $T = 10$. This suggests that, although feedback initially accelerates escape, the global minimum of the action gradually shifts to longer times as β increases. Recall from Section IIC that $\beta = 1$ denotes a bifurcation in the deterministic dynamics at which the origin $z_0 = (0, 0)$ becomes an unstable fixed point, and small fluctuations can rapidly drive the process away from it, in either direction along the x -axis. Thus, it is difficult to predict the behavior of the optimal time as $\beta \rightarrow 1$, but the saturation at $T = 10$ in Fig. 6 suggests a divergence in the optimal time, possibly due to the contribution of trajectories escaping to the left.

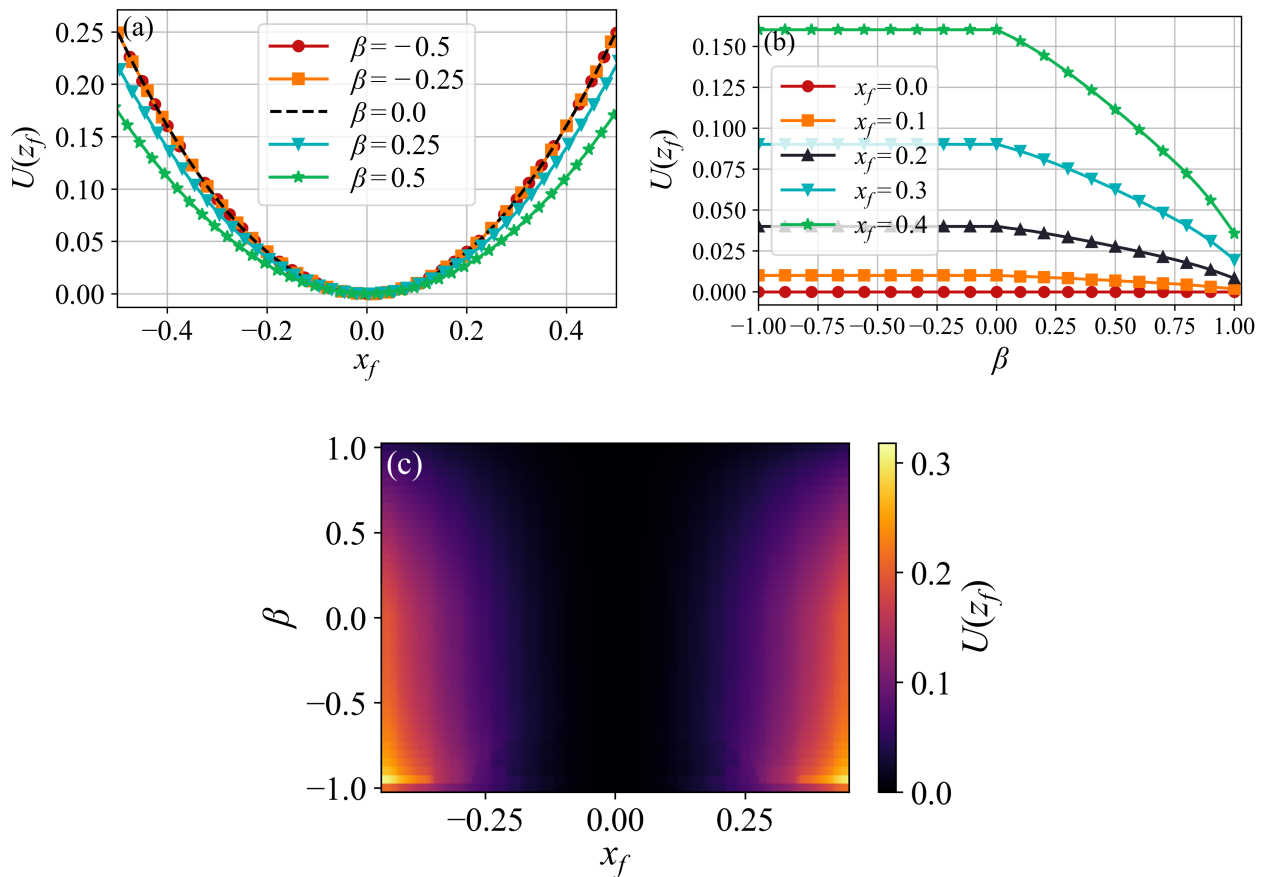


FIG. 5: (a) Quasi-potential $U(z_f)$ as a function of x_f . Curves for $\beta > 0$ lie below the OU result $U^{\text{OU}}(x_f)$, indicating that the most likely mechanism is the accumulation of positive fluctuations. For $\beta < 0$, curves collapse over $U^{\text{OU}}(x_f)$. (b) Quasi-potential $U(z_f)$ as a function of β for several values of x_f . For $\beta > 0$, the curves decrease monotonically, reinforcing the enhanced likelihood of escape via memory accumulation. For $\beta < 0$, the quasi-potential plateaus at $U^{\text{OU}}(x_f)$. (c) Heatmap of quasi-potential $U(z_f)$ as a function of x_f and β .

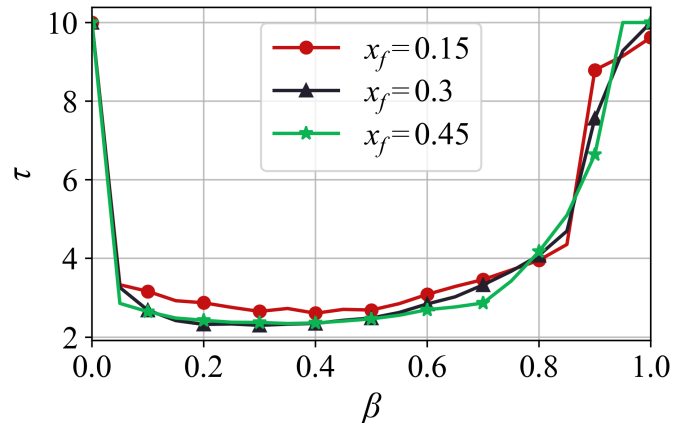


FIG. 6: Optimal escape time τ as a function of the feedback parameter β for several values of escape point x_f . For $\beta \leq 0$, τ diverges and saturates at the numerical cutoff $T = 10$. For $\beta > 0$, the optimal time becomes finite, confirming the acceleration of escape dynamics. As $\beta \rightarrow 1$, τ increases again and eventually reaches the cutoff value.

V. CONCLUSION

We have investigated the escape dynamics of an exemplary non-Markovian stochastic process. The non-Markovianity is treated by modifying a one-dimensional Ornstein–Uhlenbeck process using a time-averaged feedback wherein the drift is influenced by the empirical mean of its own trajectory. Importantly, this model belongs to the broader class of self-interacting diffusions and provides a simple, yet semi-analytically tractable, framework to study the effect of memory feedback on rare events. Beyond its theoretical appeal, such dynamics are relevant in many contexts, including feedback control systems [18] and reinforcement learning algorithms [14], where history-dependent feedback plays a central role in optimizing task execution and controlling stochastic

agents.

We used a weak-noise large deviation approach to derive the equations governing the most probable escape paths, or instantons, and characterized the associated action and quasi-potential. We found that the feedback parameter β delineates three qualitatively distinct escape mechanisms. When $\beta > 0$, escape is driven by the gradual accumulation of positive fluctuations that shift the effective potential and lead to accelerated dynamics through a reduction of the effective energy barrier. The optimal escape time, which is the time that minimizes the action, also transitions from being infinite for $\beta \leq 0$ to finite for $\beta \in (0, 1)$, providing further evidence of accelerated escape dynamics. When $\beta < 0$, escape occurs either through a slingshot-like mechanism or through an almost-ballistic trajectory, both of which are suboptimal compared to classical OU behavior. Our results establish a clear link between feedback strength and escape likelihood, showing that memory can be harnessed to fundamentally reshape the statistics of rare events.

In addition to its basic theoretical relevance, our study suggests more broadly that empirical occupation measures could act as versatile memory devices in feedback-controlled systems. In particular, we suggest that one could encode information on transient rare events into a feedback mechanism that influences future dynamics. This feedback, naturally expressible in terms of the empirical occupation measure, is especially responsive on short time scales, where it adapts quickly to new information. On longer time scales, it relaxes towards the invariant distribution, becoming progressively harder to manipulate. This feature makes it particularly suitable for capturing finite-time rare events and using that memory to modulate a system response in a closed-loop control setting, effectively guiding the process to behave in a desired manner.

Our work suggests a number of immediate questions for future research. In terms of designing systems of the type discussed in the previous paragraph, both theoretical problems and their practical implementation are of interest to pursue. For example, a compelling problem is to examine the role of finite-time window memory as a feedback mechanism. In particular, rather than considering a full-time average of the form $t^{-1} \int_0^t W(X_s, X_t) ds$, we suggest introducing a feedback based on a time-dependent finite-time window, such as $\lambda(t)^{-1} \int_{t-\lambda(t)}^t W(X_s, X_t) ds$. This formulation is truly non-Markovian and, in contrast to the model considered here, does not appear to admit a mapping to a finite-dimensional Markov system. Therefore, within the framework developed in this paper, one could also explore alternative forms of feedback, including for example those governed by the empirical variance or standard deviation of the process, rather than the empirical mean. Finally, it is of interest to analyze the effect of a changing environment by incorporating multiplicative noise, explicitly time-dependent noise or a non-autonomous deterministic backbone.

VI. ACKNOWLEDGMENTS

FC gratefully acknowledges stimulating discussions with Cristobal Arratia, Ralf Eichhorn, and Supriya Krishnamurthy at Nordita and with Baruch Meerson at Les Houches during the School ‘Theory of Large Deviations and Applications’ held in July 2024. FC is also thankful to Tobias Grafke for insightful discussions and for pointing out the correct final conditions to be used when solving Hamilton’s equations in (50). RD was supported by a scholarship from ENS Paris-Saclay (FR) during his Master 1 internship at Nordita. We acknowledge partial support from the Swedish Research Council under Grant No. 638-2013-9243 and from EPSRC under Grant No. EP/V031201/1.

REFERENCES

-
- [1] J. Beran, Y. Feng, S. Ghosh, and R. Kulik, *Long-memory processes: Probabilistic properties and statistical methods*. Springer-Verlag Berlin Heidelberg, 11 2013.
 - [2] C. Scalliet and L. Berthier, “Rejuvenation and memory effects in a structural glass,” *Physical Review Letters*, vol. 122, p. 255502, 6 2019.
 - [3] J. Zhang and T. Zhou, “Markovian approaches to modeling intracellular reaction processes with molecular memory,” *Proceedings of the National Academy of Sciences of the United States of America*, vol. 116, pp. 23542–23550, 11 2019.
 - [4] Y. M. Song, S. Campbell, L. Shiao, J. K. Kim, and W. Ott, “Noisy delay denoises biochemical oscillators,” *Physical Review Letters*, vol. 132, p. 078402, 2 2024.
 - [5] G. M. Schütz and S. Trimper, “Elephants can always remember: Exact long-range memory effects in a non-Markovian random walk,” *Physical Review E*, vol. 70, no. 4, p. 045101, 2004.
 - [6] A. Rebenshtok and E. Barkai, “Distribution of time-averaged observables for weak ergodicity breaking,” *Physical Review Letters*, vol. 99, no. 21, p. 210601, 2007.
 - [7] C. Maes, K. Netočný, and B. Wynants, “Dynamical fluctuations for semi-markov processes,” *Journal of Physics A: Mathematical and Theoretical*, vol. 42, p. 365002, 8 2009.

- [8] R. J. Harris and H. Touchette, “Current fluctuations in stochastic systems with long-range memory,” *Journal of Physics A: Mathematical and Theoretical*, vol. 42, no. 34, p. 342001, 2009.
- [9] P. V. Mieghem and R. V. D. Bovenkamp, “Non-markovian infection spread dramatically alters the susceptible-infected-susceptible epidemic threshold in networks,” *Physical Review Letters*, vol. 110, p. 108701, 3 2013.
- [10] R. J. Harris, “Fluctuations in interacting particle systems with memory,” *Journal of Statistical Mechanics: Theory and Experiment*, vol. 2015, no. 7, p. P07021, 2015.
- [11] R. L. Jack and R. J. Harris, “Giant leaps and long excursions: fluctuation mechanisms in systems with long-range memory,” *Physical Review E*, vol. 102, no. 1, p. 012154, 2020.
- [12] J. Moran, A. Fosset, D. Luzzati, J.-P. Bouchaud, and M. Benzaquen, “By force of habit: Self-trapping in a dynamical utility landscape,” *SSRN Electronic Journal*, 3 2020.
- [13] D. Hartich and A. Godec, “Emergent memory and kinetic hysteresis in strongly driven networks,” *Physical Review X*, vol. 11, p. 041047, 12 2021.
- [14] R. S. Sutton and A. G. Barto, *Reinforcement Learning: An Introduction*. A Bradford Book, 2nd ed., 1998.
- [15] J. Bechhoefer, “Feedback for physicists: A tutorial essay on control,” *Reviews of Modern Physics*, vol. 77, pp. 783–836, 7 2005.
- [16] M. L. Puterman, *Markov decision processes: Discrete stochastic dynamic programming*. Wiley, 1 2008.
- [17] S. M. Khadem and S. H. Klapp, “Delayed feedback control of active particles: a controlled journey towards the destination,” *Physical Chemistry Chemical Physics*, vol. 21, pp. 13776–13787, 6 2019.
- [18] J. Bechhoefer, *Control Theory for Physicists*. Cambridge University Press, 2 2021.
- [19] J. M. Horowitz and S. Vaikuntanathan, “Nonequilibrium detailed fluctuation theorem for repeated discrete feedback,” *Physical Review E - Statistical, Nonlinear, and Soft Matter Physics*, vol. 82, p. 061120, 12 2010.
- [20] T. Sagawa and M. Ueda, “Nonequilibrium thermodynamics of feedback control,” *Physical Review E - Statistical, Nonlinear, and Soft Matter Physics*, vol. 85, 2 2012.
- [21] Y. Jun, M. Gavrilov, and J. Bechhoefer, “High-precision test of landauer’s principle in a feedback trap,” *Physical Review Letters*, vol. 113, p. 190601, 11 2014.
- [22] S. A. Loos and S. H. Klapp, “Heat flow due to time-delayed feedback,” *Scientific Reports*, vol. 9, pp. 1–11, 2 2019.
- [23] M. Rico-Pasto, R. K. Schmitt, M. Ribezzi-Crivellari, J. M. Parrondo, H. Linke, J. Johansson, and F. Ritort, “Dissipation reduction and information-to-measurement conversion in dna pulling experiments with feedback protocols,” *Physical Review X*, vol. 11, p. 031052, 9 2021.
- [24] M. Debiossac, M. L. Rosinberg, E. Lutz, and N. Kiesel, “Non-markovian feedback control and acausality: An experimental study,” *Physical Review Letters*, vol. 128, p. 200601, 5 2022.
- [25] R. A. Kopp and S. H. L. Klapp, “Heat production in a stochastic system with nonlinear time-delayed feedback,” *Physical Review E*, vol. 110, 8 2024.
- [26] B. Tóth, “Self-Interacting Random Motions,” in *European Congress of Mathematics*, pp. 555–564, 2001.
- [27] M. Benaïm, M. Ledoux, and O. Raimond, “Self-interacting diffusions,” *Probability Theory and Related Fields*, vol. 122, no. 1, pp. 1–41, 2002.
- [28] R. Pemantle, “A survey of random processes with reinforcement,” *Probability Surveys*, vol. 4, no. 1, pp. 1–79, 2007.
- [29] P. Del Moral and L. Miclo, “Self-Interacting Markov Chains,” *Stochastic Analysis and Applications*, vol. 24, no. 3, pp. 615–660, 2007.
- [30] A. Kurtzmann, “The ODE method for some self-interacting diffusions on \mathbb{R}^d ,” *Annales de l’institut Henri Poincaré (B) Probability and Statistics*, vol. 46, no. 3, pp. 618–643, 2010.
- [31] J. Brémont, O. Bénichou, and R. Voituriez, “Exact propagators of one-dimensional self-interacting random walks,” *Physical Review Letters*, vol. 133, p. 157101, 10 2024.
- [32] F. Coghi and J. P. Garrahan, “Self-interacting processes via doob conditioning,” *arXiv: 2503.01574*, 3 2025.
- [33] E. O. Budrene and H. C. Berg, “Dynamics of formation of symmetrical patterns by chemotactic bacteria,” *Nature*, vol. 376, no. 6535, pp. 49–53, 1995.
- [34] Y. Tsori and P.-G. de Gennes, “Self-trapping of a single bacterium in its own chemoattractant,” *Europhysics Letters*, vol. 66, no. 4, p. 599, 2004.
- [35] C. R. Reid, T. Latty, A. Dussutour, and M. Beekman, “Slime mold uses an externalized spatial ”memory” to navigate in complex environments,” *Proceedings of the National Academy of Sciences of the United States of America*, vol. 109, no. 43, pp. 17490–17494, 2012.
- [36] K. Zhao, B. S. Tseng, B. Beckerman, F. Jin, M. L. Gibiansky, J. J. Harrison, E. Luijten, M. R. Parsek, and G. C. Wong, “Psl trails guide exploration and microcolony formation in *Pseudomonas aeruginosa* biofilms,” *Nature*, vol. 497, no. 7449, pp. 388–391, 2013.
- [37] W. T. Kranz, A. Gelimison, K. Zhao, G. C. Wong, and R. Golestanian, “Effective Dynamics of Microorganisms That Interact with Their Own Trail,” *Physical Review Letters*, vol. 117, no. 3, p. 038101, 2016.
- [38] B. Nakayama, H. Nagase, H. Takahashi, Y. Saito, S. Hatayama, K. Makino, E. Yamamoto, and T. Saiki, “Tunable pheromone interactions among microswimmers,” *Proceedings of the National Academy of Sciences of the United States of America*, vol. 120, no. 9, p. e2213713120, 2023.
- [39] M. Kumar, A. Murali, A. G. Subramaniam, R. Singh, and S. Thutupalli, “Emergent dynamics due to chemohydrodynamic self-interactions in active polymers,” *Nature Communications*, vol. 15, pp. 1–12, 6 2024.
- [40] W. Chen, A. Izzet, R. Zakine, E. Clément, E. Vanden-Eijnden, and J. Brujic, “Evolving motility of active droplets is captured by a self-repelling random walk model,” *Physical Review Letters*, vol. 134, p. 018301, 1 2025.
- [41] A. Budhiraja and A. Waterbury, “Empirical measure large deviations for reinforced chains on finite spaces,” *Systems & Control Letters*, vol. 169, p. 105379, 2022.
- [42] A. Budhiraja, A. Waterbury, and P. Zouboulglou, “Large Deviations for Empirical Measures of Self-Interacting Markov Chains,” *arXiv:2304.01384*, 2023.
- [43] F. Coghi, “Current fluctuations of a self-interacting diffusion on a ring,” *Journal of Physics A: Mathematical and Theoretical*, vol. 58, p. 015002, 12 2024.

- [44] A. Barbier-Chebbah, O. Bénichou, and R. Voituriez, “Self-Interacting Random Walks: Aging, Exploration, and First-Passage Times,” *Physical Review X*, vol. 12, 2022.
- [45] A. Aleksian, P. Del Moral, A. Kurtzmann, and J. Tugaut, “Self-interacting diffusions: Long-time behaviour and exit-problem in the uniformly convex case,” *ESAIM: Probability and Statistics*, vol. 28, pp. 46–61, 2024.
- [46] J. Kappler, J. O. Daldrop, F. N. Brüning, M. D. Boehle, and R. R. Netz, “Memory-induced acceleration and slowdown of barrier crossing,” *Journal of Chemical Physics*, vol. 148, 1 2018.
- [47] A. Barbier-Chebbah, O. Bénichou, R. Voituriez, and T. Guérin, “Long-term memory induced correction to Arrhenius law,” *arXiv:2406.04720*, 2024.
- [48] J. R. Norris, L. C. Rogers, and D. Williams, “Self-avoiding random walk: A Brownian motion model with local time drift,” *Probability Theory and Related Fields*, vol. 74, no. 2, pp. 271–287, 1987.
- [49] R. T. Durrett and L. C. Rogers, “Asymptotic behavior of Brownian polymers,” *Probability Theory and Related Fields*, vol. 92, no. 3, pp. 337–349, 1992.
- [50] A. Aleksian, P. Del Moral, A. Kurtzmann, and J. Tugaut, “On the exit-problem for self-interacting diffusions,” *arXiv:2201.10428v1*, 2022.
- [51] M. Benaïm and O. Raimond, “Self-interacting diffusions II: convergence in law,” *Annales de l’Institut Henri Poincaré (B) Probability and Statistics*, vol. 39, no. 6, pp. 1043–1055, 2003.
- [52] M. Benaïm and O. Raimond, “Self-interacting diffusions. III. Symmetric interactions,” *Annals of Probability*, vol. 33, no. 5, pp. 1716–1759, 2005.
- [53] M. Benaïm and O. Raimond, “Self-interacting diffusions IV: rate of convergence,” *Electronic Journal of Probability*, vol. 16, no. 66, pp. 1815–1843, 2011.
- [54] S. Chambeu and A. Kurtzmann, “Some particular self-interacting diffusions: ergodic behaviour and almost sure convergence,” *Bernoulli*, vol. 17, no. 4, pp. 1248–1267, 2011.
- [55] V. Kleptsyn and A. Kurtzmann, “Ergodicity of self-attracting motion,” *Electronic Journal of Probability*, vol. 17, no. none, pp. 1–37, 2012.
- [56] A. Aleksian, *Problème de Temps de Sortie pour les Diffusions Auto-interagissantes et Auto-stabilisantes*. PhD thesis, 2024.
- [57] J. A. Carrillo, R. J. McCann, and C. Villani, “Kinetic equilibration rates for granular media and related equations: entropy dissipation and mass transportation estimates,” *Revista Matemática Iberoamericana*, vol. 19, pp. 971–1018, 2003.
- [58] G. A. Pavliotis, *Stochastic Processes and Applications*, vol. 60. Springer New York, 2014.
- [59] W. Moon, N. J. Balmforth, and J. S. Wettlaufer, “Nonadiabatic escape and stochastic resonance,” *Journal of Physics A: Mathematical and Theoretical*, vol. 53, p. 095001, 2 2020.
- [60] W. Moon, L. T. Giorgini, and J. S. Wettlaufer, “Analytical solution of stochastic resonance in the nonadiabatic regime,” *Physical Review E*, vol. 104, p. 044130, 10 2021.
- [61] L. T. Giorgini, W. Moon, and J. S. Wettlaufer, “Analytical survival analysis of the Ornstein–Uhlenbeck process,” *Journal of Statistical Physics*, vol. 181, p. 2404–2414, 11 2020.
- [62] L. T. Giorgini, W. Moon, and J. S. Wettlaufer, “Analytical survival analysis of the non-autonomous Ornstein–Uhlenbeck process,” *Journal of Statistical Physics*, vol. 191, pp. 1–18, 10 2024.
- [63] M. I. Freidlin and A. D. Wentzell, *Random Perturbations of Dynamical Systems*. Springer, 1984.
- [64] H. Touchette, “The large deviation approach to statistical mechanics,” *Physics Reports*, vol. 478, no. 1-3, pp. 1–69, 2009.
- [65] T. Grafke and E. Vanden-Eijnden, “Numerical computation of rare events via large deviation theory,” *Chaos*, vol. 29, p. 63118, 6 2019.
- [66] M. Assaf and B. Meerson, “Wkb theory of large deviations in stochastic populations,” *Journal of Physics A: Mathematical and Theoretical*, vol. 50, p. 263001, 6 2017.
- [67] M. F. Weber and E. Frey, “Master equations and the theory of stochastic path integrals,” *Reports on Progress in Physics*, vol. 80, 3 2017.
- [68] V. I. Arnold, *Mathematical Methods of Classical Mechanics*, vol. 60. Springer New York, 1989.
- [69] H. Goldstein, C. Poole, and J. Safko, *Classical Mechanics*. 2001.
- [70] M. Schulz, *Control Theory in Physics and other Fields of Science*. Springer-Verlag, 2006.